⌘ *Author's Choice*

THE JOURNAL OF BIOLOGICAL CHEMISTRY VOL. 284, NO. 13, pp. 8395–8405, March 27, 2009

Dynamic Histone H1 Isotype 4 Methylation and Demethylation by Histone Lysine Methyltransferase G9a/KMT1C and the Jumonji Domain-containing JMJD2/KDM4 Proteins*[S]

Received for publication, October 9, 2008, and in revised form, January 12, 2009 Published, JBC Papers in Press, January 13, 2009, DOI 10.1074/jbc.M807818200

Patrick Trojer[‡§1], Jin Zhang[§2], Masato Yonezawa[¶2], Andreas Schmidt[‖], Haiyan Zheng[**], Thomas Jenuwein[¶], and Danny Reinberg[‡§3]

*From the [‡]Howard Hughes Medical Institute and [§]Department of Biochemistry, New York University School of Medicine, New York, New York 10016, [¶]IMP, Research Institute of Molecular Pathology, Vienna Biocenter, Dr. Bohr-Gasse 7, 1030 Vienna, Austria, the [‖]Department of Biochemistry, Christian-Doppler Laboratory for Proteome Analysis, University of Vienna, Vienna Biocenter, Dr. Bohr-Gasse 3, A-1030 Vienna, Austria, and the **Department of Pharmacology, Center for Advanced Biotechnology and Medicine, University of Medicine and Dentistry of New Jersey, Piscataway, New Jersey 08854*

The linker histone H1 generally participates in the establishment of chromatin structure. However, of the seven somatic H1 isotypes in humans some are also implicated in the regulation of local gene expression. Histone H1 isotype 4 (H1.4) represses transcription, and its lysine residue 26 (Lys[26]) was found to be important in this aspect. H1.4K26 is known to be methylated and acetylated *in vivo*, but the enzymes responsible for these post-translational modifications and the regulatory cues that promote H1.4 residence on chromatin are poorly characterized. Here we report that the euchromatic histone lysine methyltransferase G9a/KMT1C mediates H1.4K26 mono- and dimethylation *in vitro* and *in vivo* and thereby provides a recognition surface for the chromatin-binding proteins HP1 and L3MBTL1. Moreover, we show evidence that G9a promotes H1 deposition and is required for retention of H1 on chromatin. We also identify members of the JMJD2/KDM4 subfamily of jumonji-C type histone demethylases as being responsible for the removal of H1.4K26 methylation.

Histone lysine methyl marks have been implicated in important cellular processes including regulation of gene expression, DNA repair, cell cycle progression, cell differentiation, and recently also epigenetic processes. Despite these efforts we still do not know the substrate specificity of all histone lysine methyltransferases (HKMT)[4] (about 50 in mammals), nor do we fully comprehend the number and variety of covalent modifications and the number of potential combinatorial readouts that translate into a biological function. The recent discovery of HKDMs illustrates that methyl marks are also subject to dynamic regulation but we still lack information regarding the substrate specificity of a number of demethylases and about biological consequences of the removal of methyl marks.

In contrast to the covalent modification landscape on the core histones, post-translational modifications on the linker histone isotypes are relatively under-reported. Besides extensive histone H1 phosphorylation originally discovered in 1967 (1) and later ascribed to cell cycle regulatory events, only a handful of studies reported acetylation, methylation, ubiquitination, ADP-ribosylation, and formylation of histone H1 (2–8). This may have stemmed from the facts that H1 is dispensable in lower eukaryotes (9–11) and targeted loss of particular H1 isotypes in mammalian organisms does not show a pronounced phenotype (12–14). Knock-out of three somatic mammalian H1 isotypes, however, did lead to changes in nucleosome spacing and gene regulation (15, 16). Seven H1 isotypes are found in somatic mammalian cells, some of which are cell-type specific. Generally, H1 participates in chromatin organization and as evidenced by studies performed *in vitro* promotes the formation of condensed chromatin (17–20). However, not all H1 isotypes are functionally redundant and their roles in gene expression range from transcriptional repression to activation (21, 22) (recently discussed in Ref. 23). It seems likely that single H1 post-translational modifications or combinations thereof affect H1 chromatin binding and compaction as well as nucleosome spacing (discussed in Refs. 23 and 24).

* This work was supported, in whole or in part, by National Institutes of Health Shared Instrumentation Grants RR020932 and RR017992 (to P. L.) and National Institutes of Health Grant GM64844 (to D. R.). This work was also supported by a grant from the Howard Hughes Medical Institute (to D. R.), the Institute of Molecular Pathology (IMP) through Boehringer Ingelheim, European Union network Grant HPRN-CT 2000-00078, and the Austrian GEN-AU Initiative (financed by the Austrian Ministry of Education, Science, and Culture) (to T. J.). The costs of publication of this article were defrayed in part by the payment of page charges. This article must therefore be hereby marked "*advertisement*" in accordance with 18 U.S.C. Section 1734 solely to indicate this fact.

⌘ *Author's Choice*—Final version full access.

[S] The on-line version of this article (available at http://www.jbc.org) contains supplemental Figs. S1–S3 and Table S1.

[1] Current address: Constellation Pharmaceuticals, 148 Sidney St., Cambridge, MA 02139.

[2] Both authors contributed equally.

[3] To whom correspondence should be addressed: 522 First Ave., New York, NY 10016. Tel.: 212-263-9036; Fax: 212-263-9040; E-mail: reinbd01@nyumc.org.

[4] The abbreviations used are: HKMTs, histone lysine methyltransferases; HKDMs, histone lysine demethylases; PRC2, polycomb repressive complex 2; JmjC, Jumonji-C; cv, column volume; HA, hemagglutinin; AdoMet, *S*-adenosyl-L-methionine; MALDI, matrix-assisted laser desorption/ionization; TOF, time of flight; LC, liquid chromatography; MS, mass spectrometry; DMSO, dimethyl sulfoxide; ChIP, chromatin immunoprecipitation; DBD, DNA binding domain; PBS, phosphate-buffered saline; GST, glutathione *S*-transferase.

The first evidence for H1 lysine methylation was obtained from the analysis of the protozoan *Euglena gracilis* (25, 26). Later, the first mammalian H1 methylation site was identified on isotype 4 (also known as isotype "H1b" in human and "H1e" in mouse) at lysine 26 (H1.4K26) (5). Recently, a systematic mass spectrometric mapping of human and mouse H1 isotypes unveiled a number of mono- and dimethylated lysines on various H1 isotypes many of which are located in the globular domains (2). H1.4 confers transcriptional repression and Lys^{26} was found to be important in this context (7). We previously demonstrated that the H3K27-specific HKMT EZH2/KMT6 (27) that functions as a component of PRC2 methylates H1.4 (7, 28). In contrast, another study directed at defining the substrate preferences of PRC2 found no evidence for H1 methylation. Instead, the presence of H1 stimulated EZH2 activity toward H3K27 (29). To date there is no report describing demethylation of histone H1.

Here we used an unbiased biochemical approach to identify H1.4K26 HKMT activities. We demonstrate that G9a in addition to EZH2 methylates H1.4 *in vitro* and *in vivo* and that G9a impacts the recruitment of histone H1 to chromatin. Moreover, we use a candidate approach to identify potential H1.4K26 demethylases and find that members of the JMJD2 subfamily of JmjC-type demethylases reduce trimethylated H1.4K26 to di- and monomethylated states.

EXPERIMENTAL PROCEDURES

Conventional Purification of Histone H1.4K26 Methyltransferase Activity—HeLa nuclear pellet fraction was prepared following the protocol of Dignam *et al.* (30). Approximately 10 g of nuclear pellet fraction were subjected to 1000 ml of DE52 resin (Whatman) that was packed into a low-pressure chromatography column (15 cm diameter; Spectrum) and equilibrated with BD buffer containing 100 mM ammonium sulfate (BD-100; 20 mM Tris, pH 7.9, 0.2 mM EDTA, 2 mM dithiothreitol, 20% glycerol, 100 mM ammonium sulfate, 0.2 mM phenylmethylsulfonyl fluoride). Bound proteins were eluted by gravity flow using BD containing 350 mM ammonium sulfate (BD-350). The elution fraction was dialyzed against BD-100 and subjected to 100 ml of heparin-Sepharose 6FF (GE Healthcare) that was equilibrated with BD-100. Bound proteins were eluted with a 10-cv linear gradient from 200 to 700 mM ammonium sulfate in BD. Fractions containing H1.4K26 HKMT activity were pooled, dialyzed, and subjected to a 54-ml DEAE 5PW column (Tosoh) equilibrated with BD-100. Bound proteins were eluted with a 20-cv linear gradient from BD100 to BD800. Subsequently, fractions containing the activity were pooled, dialyzed against BD-100, and subjected to a Mono S HR10/10 (GE Healthcare) column. The elution of bound proteins was carried out as described for the DEAE 5PW step. Fractions containing activity were pooled, dialyzed against BD-100, and subjected to a Mono Q HR5/5 column (GE Healthcare). The elution of bound proteins was carried out as described for the DEAE 5PW step. Fractions containing activity were pooled and subjected to mass spectrometric analysis as well as to a Superose 6 HR10/30 gel filtration column (GE Healthcare). Fractions from the gel filtration chromatography were resolved by SDS-PAGE and visualized by silver staining or subjected to immunoblotting.

Protein Expression and Purification, Western Blot, and Silver Staining—Recombinant histone H1.4 wild type or mutant (lysine 26 changed to alanine; H1.4 K26A) was produced in bacteria as an HA-tagged fusion protein using standard techniques. Affinity purified H1.4 protein exhibited multiple bands in SDS-PAGE likely due to truncated versions of the protein. Recombinant full-length G9a was obtained using a baculoviral expression system according to standard techniques. The baculovirus containing the G9a sequence was kindly provided by Dr. Yoichi Shinkai. Baculovirally expressed GST-Jmjd2a (residues 1–506), GST-Jmjd2b (residues 1–424), GST-Jmjd2c (residues 1–372), and FLAG-Jmjd2d (residues 1–510) were purified using glutathione-Sepharose 4B (GE Healthcare) or anti-FLAG(M2) affinity gel (Sigma). Western blotting was performed using standard techniques with antibodies against HA (Sigma), FLAG(M2) (Sigma), histone H1.4K26me2 (Abcam; we find that the antibody showed a certain extent of cross-reactivity to H1.4K26me1 and -me3 in peptide dot blot experiments (supplemental Fig. S2*A*)), mouse H1.4K26me1 (Jenuwein Lab; for details of antibody generation strategy see Ref. 31), mouse H1.4K26me2/3 (7) (Jenuwein Lab) histone H1 (Santa Cruz), H3K9me1 (32) (Jenuwein Lab), H3K9me2 (Millipore), H3K9me3 (32) (Jenuwein Lab), H3K27me3 (Abcam), H3K27me2/3 (Reinberg Lab), H4K20me1 (Millipore), H4K20me3 (Millipore), H3 (Cell Signaling), GAL4 (Santa Cruz), β-actin (Ambion), GST (GE Healthcare), EZH2 (Abcam), SUZ12 (Abcam), EED (Abcam), and G9a (Yoshihiro Nakatani). Silver staining was performed using standard molecular biology methods.

In Vitro HKMT Assay—HKMT assays were carried out as described previously (33). Briefly, the reaction was performed in a total volume of 30 μl in HKMT buffer (20 mM Tris, pH 8.0, 5 mM $MgCl_2$) with 0.6 μl of 0.2 M dithiothreitol, 1 μl of [*methyl*-^{3}H]AdoMet (TRK581-1MCI, GE Healthcare), 1–10 μl of a source of enzymatic activity (either fractions of conventional purification or ~50 nM recombinant G9a), and 8 μl of substrate. The substrate consisted of ~2 μg of recombinant histone H1.4 (wild type or K26A mutant) or 5 μg of synthetic peptides corresponding to either the N terminus of histone H3 (residues 4–15) or that of H1.4 (residues 17–34). The reaction mixture was incubated for 1 h at 37 °C. HKMT assays were resolved by 15% SDS-PAGE, transferred to polyvinylidene difluoride membrane, and analyzed by fluorography using [^{3}H]ENHANCE spray (PerkinElmer Life Sciences).

In Vitro HKDM Assay—The demethylation reaction was carried out for 3–8 h at 37 °C in the presence of 30–200 ng/μl of recombinant JMJD2 proteins, 2 μM peptide substrate, 20 μM Fe(II)-sulfate, 2 μM $ZnCl_2$, 500 μM 2-oxoglutarate, 500 μM ascorbic acid, 20 mM Tris-HCl, pH 8.0, and 120–150 mM KCl in a final volume of 8 μl. To inhibit demethylation the iron chelating agent deferoxamine (Sigma) was added to a final concentration of 0.2 mM. Seventy μl of matrix solution (5 mg/ml α-cyano-4-hydroxycinnamic acid, 37% (v/v) acetonitrile, 0.12% trifluoroacetic acid) were added to the reaction products, 1 μl of the sample was spotted on a MALDI sample plate, and spectra were acquired as described (34). The following peptides were used as substrates: H3K4me3, ART[K-me3]QTARKSTGGKAPRKQL-Cys; H3K9me3, ARTKQTA-

R[Kme3]STGGKAPRKQL-Cys; H3K27me3, KAAR[Kme3]SAPATGGVKKPHRYRP-Cys; H4K20me3, SGR GKGG-[Kme3]GLGKGGAKRHRK-Cys; H1.4K26me3, PVKKKAR-[Kme3]SAGGAKRK or PVKKKAR[Kme3]AAGGAKRK; H1.4K-26me2, TPVKKKAR[Kme2]AAGGAKR-Cys; and H1.4K26me1, PVKKKAR[Kme1]SAGGAKRK.

Mass Spectrometric Analysis—Histone samples were excised from SDS-PA gels, in-gel digested with trypsin (at a w/w ratio of 1:200, trypsin:protein, estimated by the staining intensity of Coomassie Blue-stained histones) for 2 h before the reaction was stopped by addition of 5% formic acid and 60% acetonitrile. The resulting peptides were extracted and dried under vacuum. To propionylate peptides, dried digests were solubilized in 20 μl of 50 mM ammonium hydrogen carbonate followed by addition of 50 μl of a propionic anhydride solution (at a v/v ratio of 30:70, propionic anhydride:methanol) and adjustment of pH 7 with NH_4OH. The samples were incubated at 50 °C for 20 min and dried under vacuum before LC-MS/MS.

All LC-MS/MS experiments were performed using a Dionex Ultimate nanoflow HPLC system (Sunnyvale CA) and a Thermo LTQ mass spectrometer (San Jose, CA). Histone samples were first solubilized in 0.1% trifluoroacetic acid and loaded onto a trap column (Dionex Acclaim PepMap 100 C18, 5 μm, 100 Å, 300-μm inner diameter $\times$ 5 mm). After washing with 0.1% trifluoroacetic acid at 20 μl/min for 2 min, the peptides were back-flashed onto a 75 μm $\times$ 12-cm emitter column packed with Magic C18AQ, 3-μm 200 Å (Michrom Bioresources Inc., Aubum, CA), and eluted with a linear gradient of 2 to 45% acetonitrile containing 0.1% formic acid in 30 min at a flow rate of 250 nl/min. Mass spectrometry data were acquired using a data-dependent acquisition procedure with each full MS followed by analysis of the five most intense ions by a zoom scan and a MS/MS scan. Data dependent analysis used a repeat count of two and a dynamic exclusion duration of 60 s.

Transfections, Stable Cell Line—3 $\times$ 10^6 293T cells were transfected with 10 μg of plasmid DNA using FuGENE HD (Roche) according to the manufacturer's instructions. Cells were incubated for 48 h post-infection, harvested, and whole cell extract prepared using RIPA buffer (10 mM Tris, pH 7.4, 150 mM NaCl, 1% Nonidet P-40, 0.5% deoxycholic acid, 0.1% SDS, 1 mM EDTA). Alternatively, transfected cells were subjected to histone extraction. The generation of the NIH3T3-tet off cells (Clontech) with a stably integrated, inducible Jmjd2b(1–424)-green fluorescent protein expression construct was described previously (35). Induction was performed for 12 h and green fluorescent protein-positive cells were fluorescence-activated cell sorter-sorted and histones extracted.

Histone Extraction—Core and linker histones were extracted from 293, 293FT, HeLa, 293TREx-luciferase (see below), NIH 3T3, and embryonic stem cells using 0.2 M sulfuric acid according to standard protocols. The acidic supernatant (containing histones) was neutralized by the addition of 0.75 volume of 1.5 M Tris, pH 8.8. Cells were either untreated or treated with the G9a small molecule inhibitor BIX-01294 (kindly provided by Boehringer Ingelheim Pharmaceuticals, Inc.) or the histone deacetylase inhibitor trichostatin A (Sigma).

Immunoprecipitation—One mg of solubilized nuclear pellet was mixed with 1 volume of BD-200 plus 0.05% Nonidet P-40. Five μg of antibody were added and the reaction mixture (~200 μl) incubated overnight at 4 °C on a rotating wheel. Twenty μl of pre-equilibrated protein G-agarose (Roche) were added and incubation continued for 1 h at 4 °C on a rotating wheel. Reactions were spun in a microcentrifuge at 400 $\times$ *g* for 3 min, the supernatant was discarded, and beads washed two times with 400 μl of BC-200 containing 0.05% Nonidet P-40, one time with 400 μl of BC-500, 0.05% Nonidet P-40, followed by one time with 400 μl of BC-100. Beads were mixed with Laemmli sample buffer and analyzed by SDS-PAGE.

Reverse Transcriptase-PCR—HeLa cells were grown in the presence of 1% DMSO or 2.5 μM decitabine (5-*aza*-2′-deoxycytidine) in DMSO for 72 h. Total RNA was isolated using TRIzol® (Invitrogen) and cDNA was produced using the SuperScript III cDNA synthesis kit according to the manufacturer's instructions. Real time PCR was performed using the Brilliant® II SYBR® Green QPCR Master Mix (Stratagene). Primer sequences are available upon request.

ChIP—We previously generated a 293 TREx cell line (Invitrogen) that is stably transfected with a constitutively expressing luciferase transgene containing GAL4 DNA binding sites upstream of the transcriptional start site (293TREx-luciferase (8)). This cell line was stably transfected with pcDNA4TO (Invitrogen) containing the GAL4-DBD and full-length cDNA of human G9a (inserted between the HindIII and EcoRI sites). GAL4-tagged G9a was expressed upon addition of 2 μg/ml tetracycline/doxycycline for 24 or 48 h. ChIP was performed in duplicate according to standard techniques and as previously described (36) using the following primer set: upper, 5′-CACCGAGCGACCCTGCATAAGC-3′ and lower, 5′-GCTTCTGCCAACCGAACGGAC-3′. Briefly, cells were treated with 1% formaldehyde in the growth medium for 10 min at room temperature. Cross-linking was quenched by the addition of glycine to a final concentration of 125 mM in growth medium. Cells were washed twice with phosphate-buffered saline and lysed in buffer A (25 mM Tris, pH 8.0, 1% SDS, 1 mM EDTA, 25 mM NaCl). Cell lysate was sonicated using a Bioruptor™ 200 (Diagenode) with 200 watts ultrasonic wave output power. Sonication was carried out for 15 min with alternating 30-s on/off pulses. Sheared chromatin was used for immunoprecipitation using antibodies described above and antibodies against GAL4 (Millipore) and random IgG (Jackson). H1.4K26me2 antibody competition with histone peptides was carried out as follows: 5 μg of antibody was mixed in a tube with 1 μM H3K9me2, H1K26me0, and H1K26me2 peptides in a final volume of 40 μl for 30 min on ice. The entire mixture was subsequently used for ChIP. Precipitated material was analyzed by real time quantitative PCRs carried out in triplicate. Paired *t*-tests were performed to calculate *p* values. ChIP experiments on the endogenous *MAGE-A1* promoter were carried out in triplicate as described above using HeLa cells grown in the presence or absence of 2.5 μM decitabine for 72 h. The following primer set was used: oligo 1, 5′-GTCCAGGCTCTGCCAGACATC-3′ and oligo 2, 5′-CGTCCCTCAGAATGGAAACCTC-3′. The *GAPDH* ChIP primer set is located around the transcriptional start site and the sequence is available upon request.

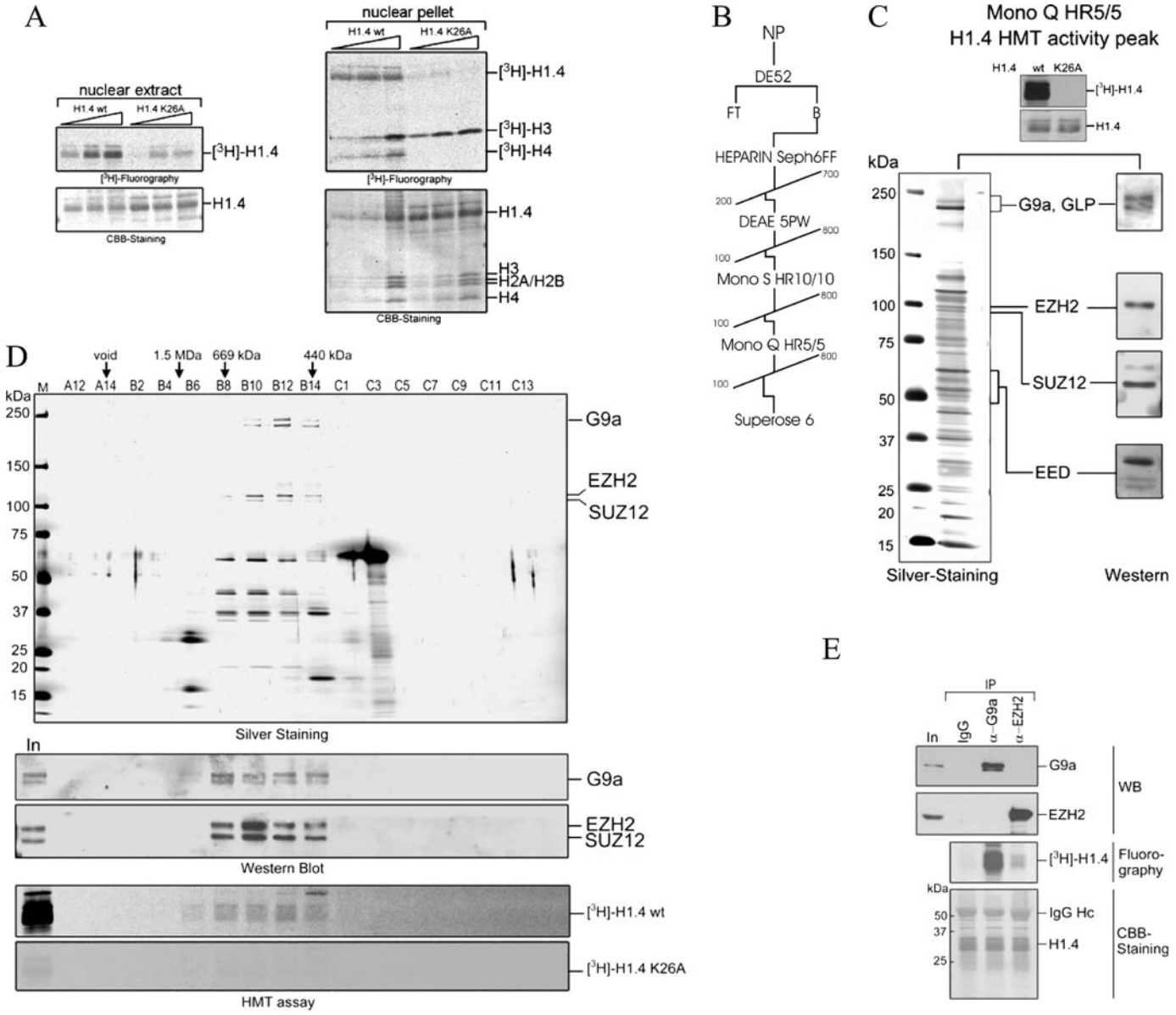

FIGURE 1. **Purification of H1.4K26 HKMT activities from HeLa nuclear pellet.** *A*, HKMT assays carried out with increasing amounts of nuclear extract (*left*) or nuclear pellet (*right*) using recombinant wild type histone H1.4 or a version with a Lys[26] to Ala point mutation as substrate. *B*, purification strategy to isolate H1.4K26-specific HKMT activities. *C*, Mono Q peak fraction of H1.4K26 HKMT activity was analyzed by SDS-PAGE and silver staining (*left*). Specificity is illustrated by HKMT assay using wild type or K26A mutant H1.4 as substrate (*top*). The fraction was subjected to mass spectrometric analysis and identified HKMTs were confirmed by immunoblotting (*right*). *D*, H1.4K26 HKMT activity peak from the Mono Q step was pooled and subjected to a Superose 6 gel filtration column. Fractions were either analyzed by HKMT assay or resolved by SDS-PAGE and analyzed by silver staining or immunoblotting. HKMT assays were performed using wild type or K26A mutant H1.4 as substrate. *E*, immunoprecipitation experiment from nuclear pellet fraction using IgG, anti-G9a, and anti-EZH2 antibodies. Precipitated material was analyzed by HKMT assays or immunoblotting.

RESULTS

Purification of H1.4K26 Methyltransferase Activities—We, and others previously reported that H1.4K26 is methylated *in vivo* (2, 5, 7). In an unbiased attempt to identify H1.4K26-specific methyltransferases we used recombinant bacterially expressed histone H1.4 as a substrate for *in vitro* HKMT assays and readily detected the H1-specific HKMT activity in both nuclear extract and pellet fractions. The target specificity of the HKMT activity assays was verified by comparing methylation of wild type H1.4 to that of a version in which the Lys[26] residue was mutated to alanine (H1.4K26A) (Fig. 1*A*). Notably, methylation of the K26A mutant was strongly reduced but not completely abolished, suggesting that other residue(s) on histone H1.4 in addition to Lys[26] are methylated. The endogenous core histones H3 and H4 were methylated when the nuclear pellet fraction was used in HKMT assays. Surprisingly, the addition of recombinant H1.4K26A but not wild type H1.4 abolished the activity toward H4. At present we do not know if this finding is relevant and did not pursue it further in this study.

We next performed a conventional purification from the nuclear pellet following H1.4 HKMT activity (Fig. 1*B*) and found that H1.4K26-specific and non-Lys[26]-specific activities co-eluted throughout the entire purification (supplemental Fig. S1*A* and data not shown). The peak fraction of the Mono Q

elution (Fig. 1*C*) was subjected to mass spectrometric analysis. Among other polypeptides we identified three HKMTs: G9a/KMT1C, GLP/KMT1D, and EZH2/KMT6 and the presence of each was verified by Western blot (Fig. 1*C* and supplemental Table S1). Analysis of the H1.4K26 HKMT activity by gel filtration chromatography revealed that the activity peak migrated at high molecular mass (400–800 kDa) and correlated well with both the G9a and EZH2 elution profiles as visualized by Western blot (Fig. 1*D*). Interestingly, a larger migrating H1.4 protein species was mainly methylated in fraction B14 and its radiolabel intensity did not correlate with the G9a and EZH2 elution profiles. Although fraction B14 contained G9a and EZH2, it is unclear why its substrate preference was different from that of fractions B8–B12. The methylation on this H1.4 protein was also Lys^{26} specific because the radiolabel was lost when the fractions were assayed with an H1.4K26A mutant protein (Fig. 1*D*).

We demonstrated previously that EZH2 was able to methylate H1.4. Therefore, it was possible that EZH2 is solely responsible for the H1.4 methylation observed. To clarify this we performed immunoprecipitations from nuclear pellet fractions and demonstrated that: 1) G9a and EZH2 do not interact; 2) both G9a and EZH2 immunoprecipitates contain H1.4 HKMT activity compared with an IgG control (Fig. 1*E*); and 3) the presence of histone octamers in the HKMT assay does not abolish G9a activity toward H1.4 (supplemental Fig. S1*B*). Significantly less activity is precipitated with anti-EZH2 but this might be explained by the fairly stringent wash conditions that partially disrupted the EZH2 containing PRC2 complex.

G9a Methylates H1.4 at Lysine 26—Given that G9a was shown previously to methylate native histone H1 *in vitro* (37) we used recombinant full-length G9a to perform *in vitro* HKMT assays with either wild type H1.4 or its K26A mutant as substrate. We detected significant $[^3H]CH_3$ incorporation on wild type H1.4 as evidenced by fluorography (Fig. 2*A*) but a signal was not detected on H1.4K26A. However, longer exposure times gave evidence of minor $[^3H]CH_3$ label (data not shown) suggesting that other lysines might be methylated with low efficiency. The reaction was carried out in substrate excess to attain the maximum amount of methylation under the given assay conditions to facilitate mass spectrometric analysis (see Fig. 2*D*). We monitored the increase in Lys^{26} methylation upon incubation of HA-tagged H1.4 with G9a and AdoMet using anti-H1.4K26me2-specific antibody (Fig. 2*B*). Importantly, the antibody was methyl-specific because recombinant un-methylated H1.4 was not recognized despite being recognized by an anti-HA antibody (Fig. 2*B*). The multiple bands are recognized by anti-HA and anti-H1.4K26me2 antibodies likely resulted from H1.4 truncations (see "Experimental Procedures"). Next, we used synthetic peptides corresponding to residues 17–34 of H1.4 that were either unmethylated or harbored one, two, or three methyl groups at Lys^{26} as substrates for G9a-dependent HKMT assays. G9a only utilized unmethylated and monomethylated peptides in a time-limiting reaction, similar to the result obtained when H3K9-peptides were used as substrate (Fig. 2*C*). Therefore, G9a predominantly functions as an H3K9 and H1.4K26 mono- and dimethylase *in vitro*, although extended incubation times allowed G9a to perform trimethylation of the substrate (data not shown; previously discussed in Ref. 38).

G9a-methylated H1.4 was subjected to mass spectrometry to unambiguously identify target sites. Due to the high lysine content of H1.4 the sample was propionylated before digestion to better distinguish mass differences in LC-MS/MS. The mass spectra of recombinant H1.4 incubated with G9a in the presence of AdoMet resulted in the detection of peptides with mono- and dimethylated H1.4K26 (Fig. 2*D*, *middle* and *bottom panels*, spectra shown in *black*). In the absence of G9a or AdoMet, peptides with methylation on Lys^{26} were not detected (Fig. 2*D*, *top panel*, spectra shown in *black* and *red*, *middle* and *bottom panels*, spectra shown in *red*). In addition to H1K26 we found minor amounts of methyl groups incorporated on several other lysine residues (Fig. 2*E*) none of which were considered relevant at this point.

G9a Methylates H1.4 at Lysine 26 in Vivo—We next tested if G9a impacted H1.4K26 methylation in cell-based assays. To this end we extracted histones from cells transiently expressing G9a fused to a GAL4-DBD. Overproduction of G9a significantly increased global H1.4K26 dimethylation and also moderately increased the level of H3K9me2. GAL4-DBD alone or fused to the H4K20-specific HKMT PR-SET7/KMT5A did not alter H1.4K26me2 or H3K9me2 levels (Fig. 3*A*). Previous reports indicated that the lack of G9a substantially reduced H3K9me2 and -me1 in mouse embryonic stem cells (32, 39, 40). We extracted core and linker histones from these wild type and $G9a^{-/-}$ stem cell lines (TT2 and 2210, respectively), and observed a global reduction in H1.4K26me2 in the case of $G9a^{-/-}$ cells as visualized by Western blot (Fig. 3*B*).

To demonstrate by alternative means that G9a is partially responsible for H1.4K26 methylation *in vivo* we took advantage of a recently identified, small molecule inhibitor of G9a. The compound termed BIX-01294 is specific for G9a as even the highly homologous GLP protein is far less effectively inhibited (41). HeLa cells were treated for 48 h with BIX-01294 at a final concentration of 9 μM, histones were extracted and analyzed by Western blot. Inhibition of G9a led to significant decreases in H1.4K26me2 and H3K9me2 levels (Fig. 3*C*), whereas other histone lysine methylation marks were unaffected (Fig. 3*C* and data not shown). Interestingly, trichostatin A-treated cells also showed a considerable reduction in global H1.4K26me2 levels. Previously, we demonstrated that H1.4K26 is acetylated *in vivo* and that the class III histone deacetylase SIRT1 targeted H1.4K26 (8). Now, our data suggest that Lys^{26} is also targeted by class I and II histone deacetylases and that acetylation of H1.4K26 might protect it from being methylated.

G9a Methylates H1.4K26 on Chromatin in a Gene-specific Manner—Generally, histone H1 deposition condenses chromatin structure and negatively regulates gene expression, although various histone H1 isotypes seem to affect transcription differently (recently reviewed in Ref. 23). As histone H1.4 repressed transcription in reporter gene assays (7), we tested if G9a and H1.4 can co-occupy repressed genes. To this end a 293 cell line was stably transfected with a construct encoding GAL4-DBD fused in-frame to G9a (GAL4-G9a) under the control of a promoter that contains a Tet-operator sequence. In the default state (−Tet) GAL4-G9a expression is suppressed. Upon

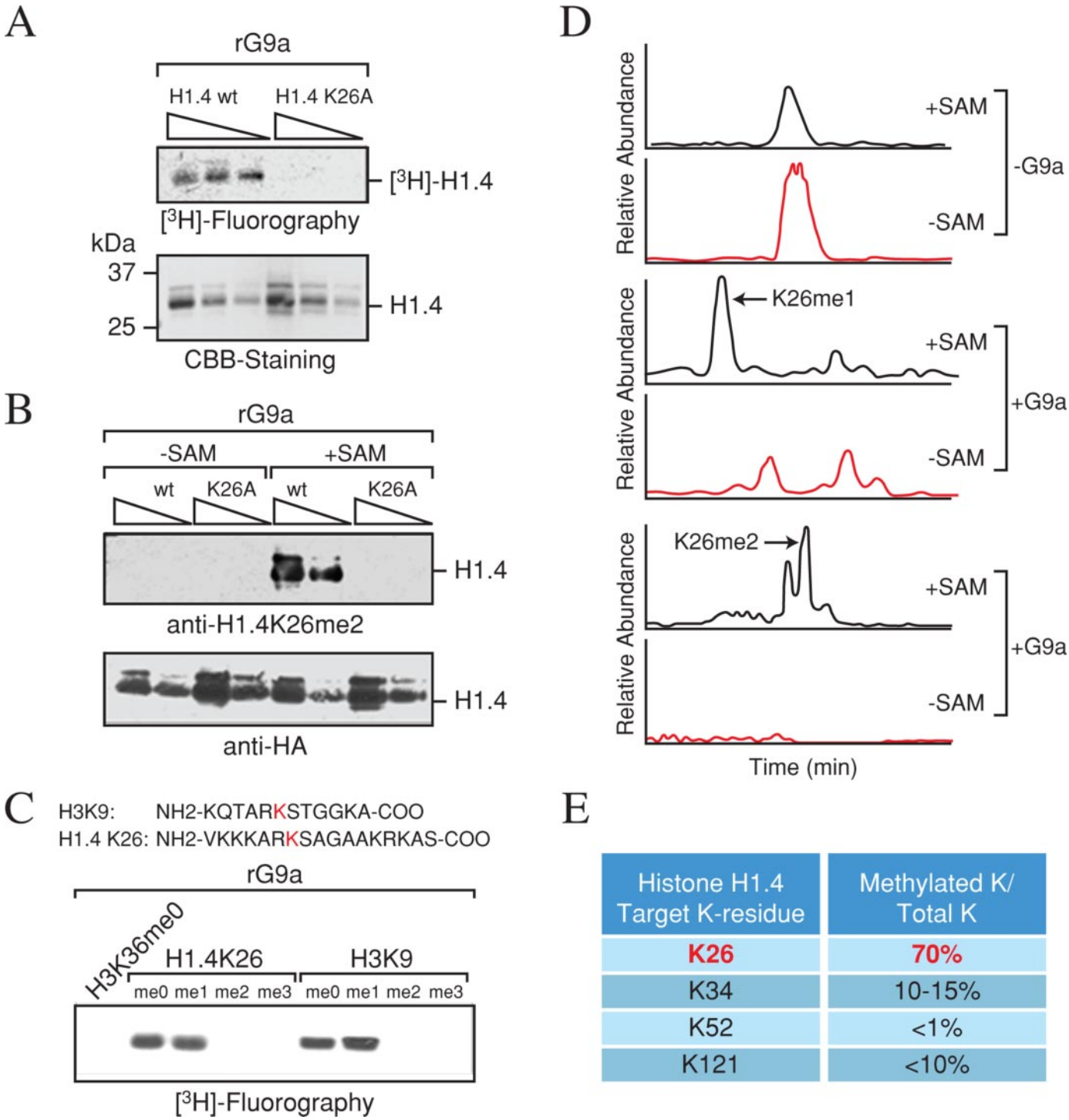

Histone H1.4 Target K-residue	Methylated K/ Total K
K26	**70%**
K34	10-15%
K52	<1%
K121	<10%

FIGURE 2. **Recombinant G9a methylated H1.4 at Lys^{26} *in vitro*.** *A*, recombinant full-length G9a derived from a baculoviral expression system was used to methylate increasing amounts of recombinant wild type or K26A mutant HA-tagged H1.4 using ^{3}H-labeled AdoMet as methyl donor. Shown is the fluorography after an exposure time of 12 h (*top panel*) and the Coomassie Blue-stained membrane to visualize the amount of H1.4 and H1.4K26A proteins (*bottom panel*). *B*, as in *A* but using unlabeled AdoMet as methyl donor. Detection of methyl groups incorporated at H1.4K26 was carried out by Western blot using a specific anti-H1.4K26me2 antibody. An anti-HA antibody was used to determine the total H1.4 levels. *C*, as in *A* but using synthetic peptides corresponding to the sequence shown for H1.4 or H3 (*top*) as substrate. HKMT assay incubation time was limited to 30 min. *D*, recombinant wild type H1.4 was incubated with G9a in the presence or absence of unlabeled AdoMet as methyl donor. The reactions were resolved by SDS-PAGE, stained with Coomassie Brillant Blue, and the H1.4 bands then cut from the gel and subjected to mass spectrometry. Ion chromatograms of ^{26}KKSAGAAR peptides are shown with different modifications generated from LC-MS/MS data of propionylated partial tryptic digest of histone H1.4. Only the sample incubated with G9a and AdoMet led to the detection of monomethylated ($[M + 2H]^{2+} = 578.1$) and dimethylated Lys^{26} ($[M + 2H]^{2+} = 557.2$) (spectra shown in *black*). Only unmodified H1.4K26 peptides were detected in the absence of AdoMet (spectra shown in *red*). In the absence of G9a only unmodified ($[M + 2H]^{2+} = 570.8$) Lys^{26} peptides were detected. *E*, the table summarizes other potential H1.4 target sites and the percentage of methylation compared with an unmethylated H1.4 control.

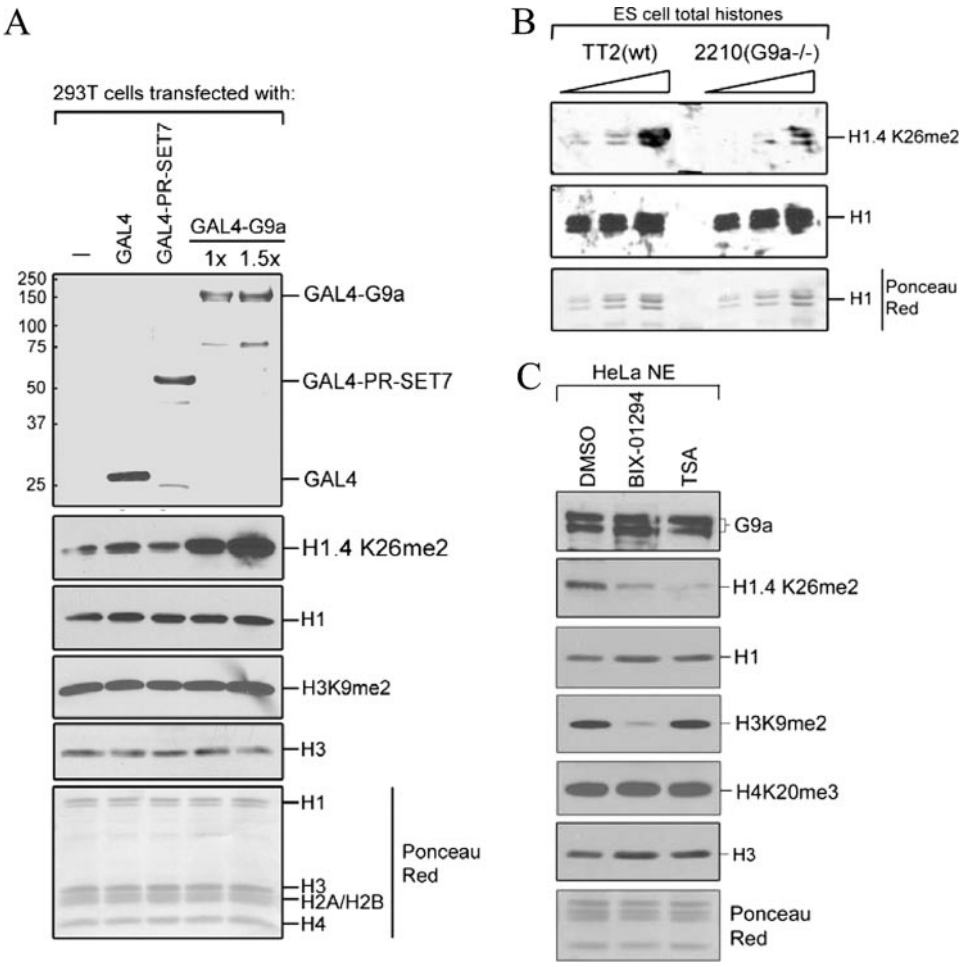

FIGURE 3. **G9a methylates H1.4K26 *in vivo*.** *A*, 293T cells were transiently transfected with GAL4, GAL4-PR-SET7, or GAL4-G9a. Whole cell extract was prepared from transfected cells or acid extraction was performed to isolate core and linker histones and both fractions were analyzed by Western blot using antibodies indicated on the *right*. Anti-GAL4 was used for the *top panel*. *B*, acid extraction of histones was performed from wild type (*TT2*) or G9a$^{-/-}$ (*2210*) embryonic stem cells and purified histones were analyzed by Western blot using antibodies indicated on the *right*. *C*, 293T cells were treated for 48 h with DMSO, compound BIX-01294 (a specific G9a inhibitor; final concentration 9 μM), or trichostatin A (final concentration 300 nM). High salt nuclear extracts were prepared from treated cells and analyzed by Western blot using the antibodies indicated on the *right*.

addition of doxycycline (+Tet) GAL4-G9a protein binds to GAL4-specific DNA binding sites integrated in the promoter of the luciferase reporter gene (Fig. 4*A*). GAL4-G9a strongly repressed luciferase expression (Fig. 4*B*) consistent with earlier reports that described G9a as a transcriptional co-repressor (39–42). Induction of GAL4-G9a expression for 48 h was monitored by a significant increase in GAL4-G9a protein as well as by a global increase in H1.4K26me2 and H3K9me2 levels (Fig. 4*C*).

To determine whether G9a-mediated luciferase repression correlates with H1 deposition and H1.4K26 methylation we performed ChIP experiments. As expected, GAL4-G9a was recruited to the promoter region of the luciferase gene in the presence of doxycycline. Interestingly, histone H1 occupancy was low on the luciferase gene but increased upon luciferase repression by GAL4-G9a. Moreover, the levels of H3K9me2 and H1.4K26me2 increased in the presence of doxycycline, whereas those of H3K27me3 remained unchanged (Fig. 4*D*). To rule out that the H1.4K26me2-specific antibody used for ChIP cross-reacted with H3K9me2 we performed peptide competition experiments. Dot blot analysis confirmed that the anti-H1.4K26me2 antibody specifically recognized H1.4 peptides but not H3K9, H3K27, or H4K20 peptides. Moreover, the recognition of H1.4K26me2 could be abolished only upon preincubating anti-H1.4K26me2 antibodies with H1.4K26me2 peptides, but not with H3K9me2 or H3K27me2 peptides (supplemental Fig. S2). We repeated the ChIP with H1.4K26me2 antibodies that were competed with various histone peptides prior to the immunoprecipitation step. Analysis of precipitated material by real time-quantitative PCR showed that H3K9me2 and H1.4K26me0 peptides did not significantly reduce the amount of precipitated material ($p > 0.05$). Of note, an H3K9me2-specific antibody was completely neutralized by the H3K9me2 peptide under identical conditions. Competition with H1.4K26me2 peptides reduced significantly the signal intensity as determined by paired *t*-tests ($p < 0.05$; Fig. 4*E*). The fact that the H1.4K26me2 peptide did not fully abolish the signal indicates that the antibody shows a low level of cross-reactivity.

Results from the ChIP experiments on the luciferase transgene suggest that G9a alters the chromatin structure by promoting the recruitment of H1. To test this hypothesis on an endogenous gene we focused on *MAGE-A* genes, previously shown as being occupied by G9a and with its presence being linked to gene silencing (39). *MAGE-A* gene silencing is also mediated by DNA methylation in a number of tumor cell lines. It is well established that global and gene-specific DNA methylation decreases upon addition of the cytosine analog decitabine. Treatment with decitabine was previously shown to reactivate tumor suppressor genes, with G9a occupancy at these genes being substantially reduced (44). We selected *MAGE-A1* for a comparative ChIP analysis before and after addition of decitabine. In the absence of decitabine, G9a and histone H1 were present on the *MAGE-A1* gene and H1.4 was methylated at Lys^{26} (Fig. 4*G*). Despite that *MAGE-A* transcripts are detectable in HeLa cells (43) we found *MAGE-A1* and *-A3* gene expression to be induced upon treatment with decitabine (Fig. 4*F*). As well, G9a was lost from the *MAGE-A1* promoter region and importantly, the levels of H1K26 methylation were also reduced, presumably due to the decrease in total H1 protein. These results are in accord with those obtained using the luciferase reporter gene above, suggesting that G9a promotes spatially restricted H1 residency on chromatin.

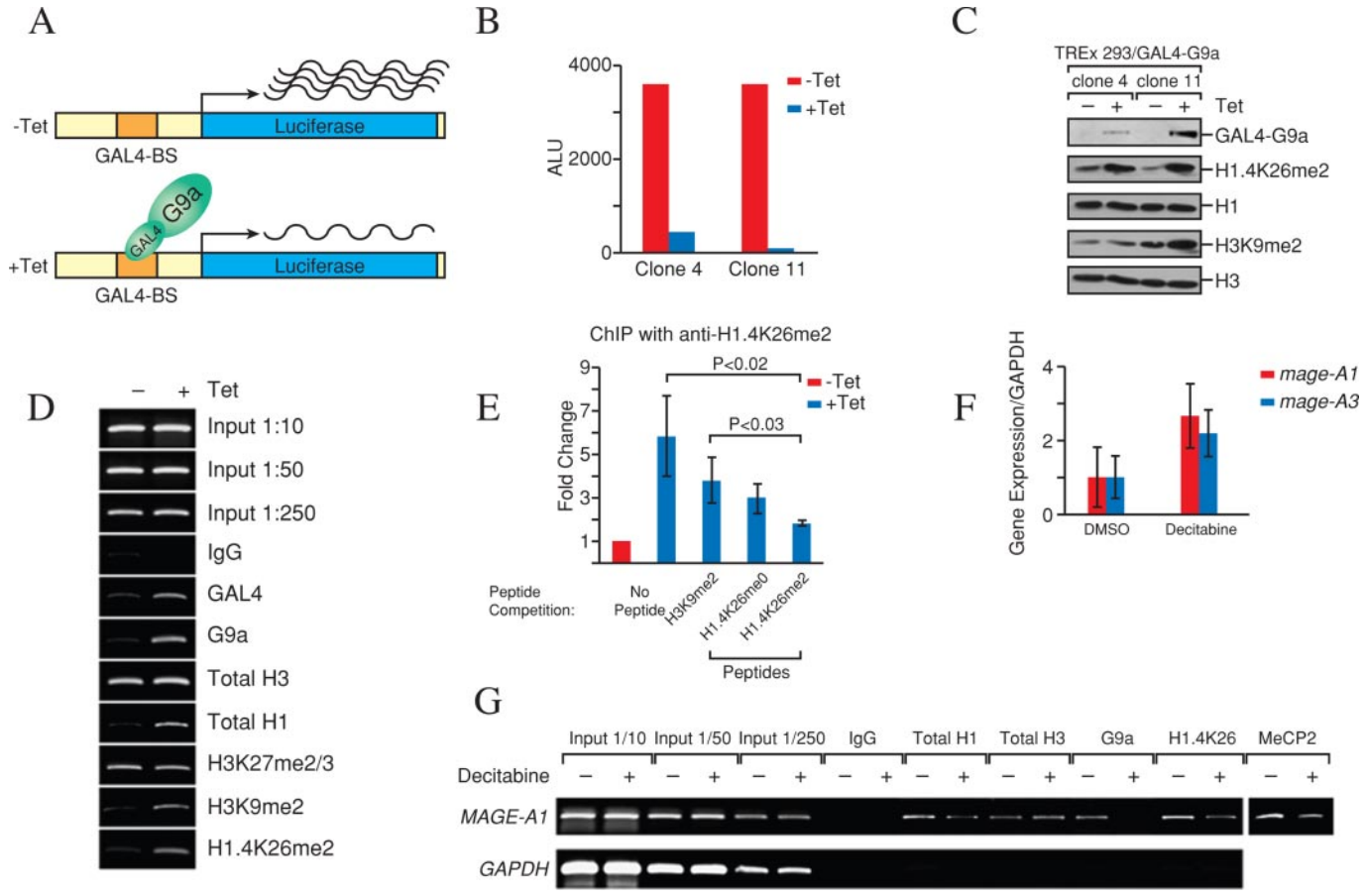

FIGURE 4. **G9a methylates H1.4K26 on a specific genomic location and promotes H1 recruitment.** *A*, illustration of the transgene system that allows tetracycline-induced expression of GAL4-G9a and targeting to the luciferase promoter containing GAL4 DNA binding sites. Notably, luciferase is constitutively expressed in the default state (−Tet). *B*, induction of GAL4-G9a effectively represses luciferase expression as demonstrated by luciferase assays of two independent clones. The experiments were carried out in duplicate and the result of one representative experiment is shown. *C*, whole cell extracts were prepared from two independent clones that were grown in the absence or presence of tetracycline for 24 h. Extracts were analyzed by Western blot using the antibodies indicated on the *right*. *D*, ChIP experiments from cells grown in the absence or presence of tetracycline for 24 h. Antibodies used for the ChIPs are indicated on the *right*. One representative of two independent experiments is shown. *E*, ChIPs with anti-H1.4K26me2 antibodies either untreated or preincubated with synthetic peptides corresponding to various histone sequences and modification states. Quantitative real time PCR analysis for each sample was carried out in triplicate. *p* values are indicated and were calculated by paired *t*-tests. Competition with H3K9me2 and H1.4K26me2 peptides did not result in statistically relevant ($p > 0.05$) reduction of PCR product. *F*, quantitative real time RT-PCR measuring *MAGE-A1* and *-A3* transcript levels from HeLa cells treated for 72 h with DMSO or decitabine. The *GAPDH* transcript level was used for normalization. Three biological replicates were used and all PCR were performed in triplicate. *G*, ChIP experiments carried out from 293 cells analyzing the *MAGE-A1* promoter in the absence or presence of decitabine. ChIP at the *GAPDH* gene served as a negative control. One representative of three independent experiments is shown.

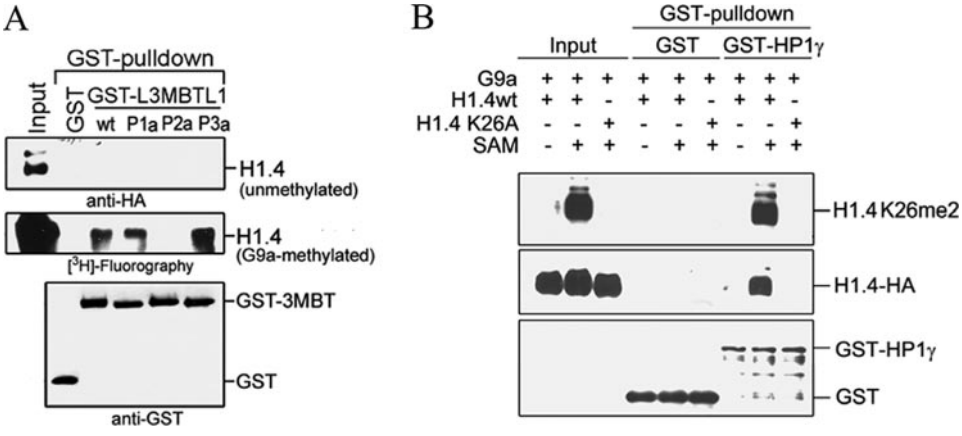

FIGURE 5. **G9a-methylated H1.4 is recognized by L3MBTL1 and HP1γ *in vitro*.** *A*, GST pull-down experiment with GST or GST fused to the three MBT domains of L3MBTL1 (GST-3MBT) and recombinant HA-tagged H1.4 either unmethylated or methylated by G9a. Notably, a point mutation in the second MBT domain (*P2a*) abolished binding but mutations in the first and third MBT domains (*P1a* and *P3a*) retained binding to G9a-methylated H1.4. Methylated H1.4 was visualized by ^{3}H-fluorography. *B*, GST pull-down experiment with GST or GST-HP1γ and recombinant HA-tagged H1.4 either unmethylated or methylated by G9a. Methylated H1.4 was visualized by Western blot using anti-H1.4K26me2 antibodies.

H1.4 Methylated at Lys^{26} by G9a Provides a Binding Surface for L3MBTL1 and HP1—Chromodomain-containing HP1 and MBT domain-containing L3MBTL1 proteins were previously shown to specifically recognize methylated H1.4 (36, 45). To examine if G9a is able to mediate this binding event we performed pull-down assays using recombinant H1.4 that was pre-methylated by G9a. A GST fusion protein comprising the three MBT domains of L3MBTL1 co-precipitated with methylated, but not unmethylated H1.4. We previously showed that the second MBT domain was responsible for methyllysine binding (36) and indeed a

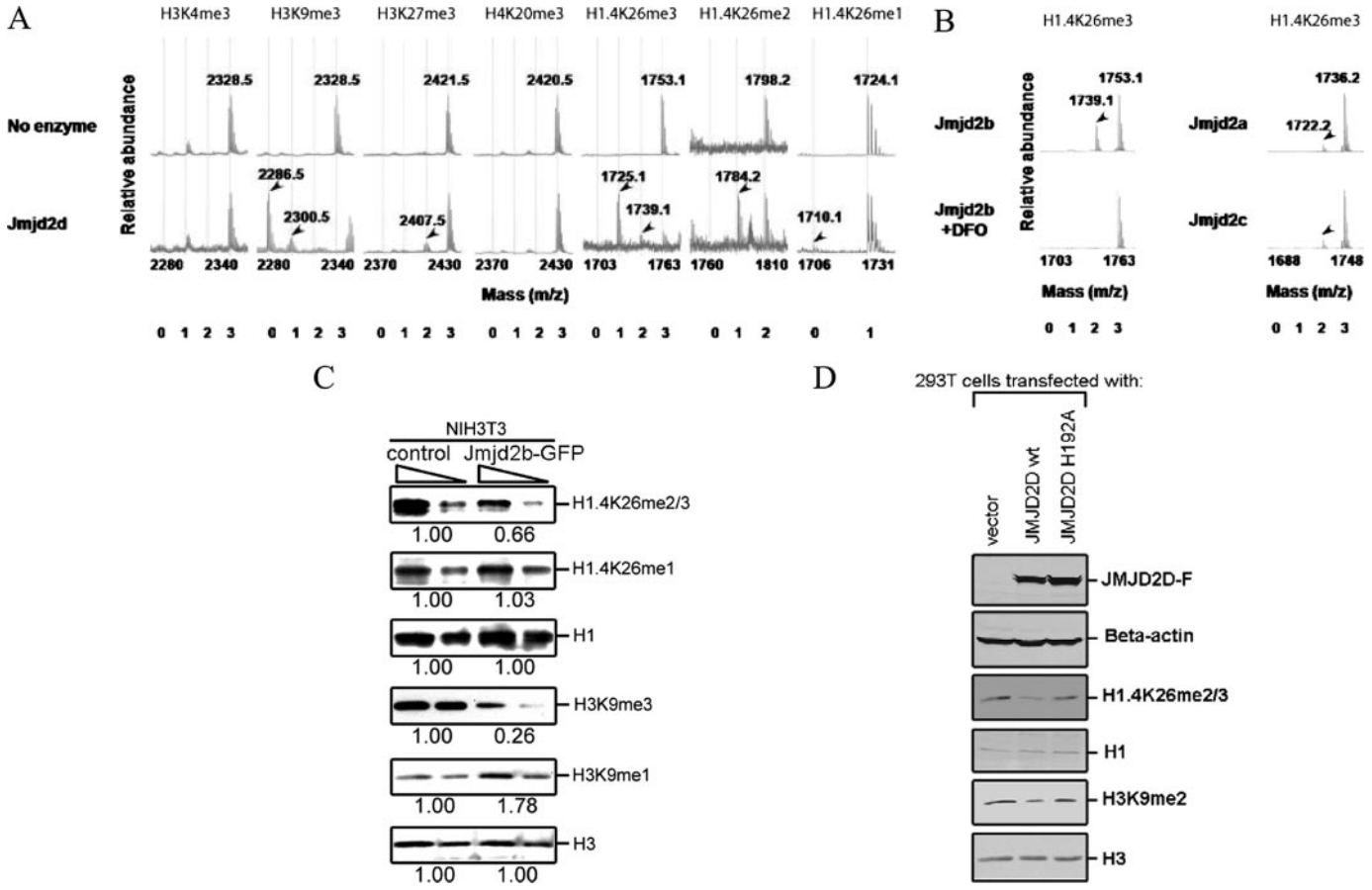

FIGURE 6. **Members of the JMJD2 subfamily of the JmjC domain-containing proteins demethylate H1.4K26 *in vitro* and *in vivo*.** *A*, identification of mouse Jmjd2d H1.4K26 demethylase activity by MALDI-TOF mass spectrometry. Each panel contains a spectrum for H3K4me3, H3K9me3, H3K27me3, H4K20me3, H1.4K26me3, H1.4K26me2, and H1.4K26me1 peptides incubated with or without mouse Jmjd2d protein. The masses corresponding to unmodified (*0*), mono- (*1*), di- (*2*), or trimethylated (*3*) peptides are indicated in *dotted lines*. The appearance of a peak corresponding to the demethylated peptide is marked with an *arrowhead*. The shift corresponds to a loss of 14, 28, or 42 daltons due to the removal of methyl group(s). *B*, Jmjd2a, Jmjd2b, and Jmjd2c were also identified as H1K26me3 demethylases. Addition of the iron chelator deferoxamine at the beginning of the reaction suppressed the formation of a demethylated peptide peak. *C*, NIH3T3 cells stably expressing mouse Jmjd2b display a reduction in H1.4K26me2/3 and H3K9me3. Total H1 and H3 levels served as a loading control. Acid-extracted histones (1 or 2 μg) were analyzed as indicated by *triangles* on the *top*. *D*, ectopic expression of human JMJD2D wild type but not its catalytic point mutant (H192A) in 293T cells causes global reduction in H1.4K26me2/3 and H3K9me2. β-Actin, total H1, and total H3 served as loading controls.

point mutation in the second (P2a) but not in the first or third (P1a, P3a) MBT domains abolished the interaction with G9a-methylated H1.4 (Fig. 5*A*). Similarly, GST-HP1γ but not GST alone interacted with G9a-methylated H1.4 (Fig. 5*B*). Importantly, unmethylated H1.4 was not precipitated when G9a was added to the pull-down assay, ruling out the possibility that G9a bridges the interaction between H1.4 and HP1γ.

Identification of H1.4K26 Demethylases—Candidate approaches have been useful to identify the targets of the JmjC domain-containing histone lysine demethylases. We, and others previously identified JMJD2 proteins to specifically demethylate H3K9 and H3K36 (34, 35, 46, 47). Here, we tested a large panel of JmjC proteins among which JMJD2 proteins exhibited significant activity toward methylated H1.4K26. We purified recombinant mouse JMJD2 proteins from baculovirus-infected Sf9 cells (supplemental Fig. S3) and examined demethylase activity toward methylated H1.4K26 peptides along with trimethylated H3K4, H3K9, H3K27, and H4K20 peptides. Recombinant Jmjd2d efficiently converted H1.4K26me3 and H1.4K26me2 to the monomethyl state as detected by MALDI-TOF mass spectrometry, whereas conversion of an H1.4K26me1 peptide substrate to the unmethylated state was inefficient (Fig. 6*A*). Conversion of H1.4K26me3 to the monomethylated state is consistent with the previous observation that human JMJD2D removes two methyl moieties from trimethylated H3K9 (35, 47). Under the assay conditions used in Fig. 6*A* complete H3K9 demethylation was observed due to the relatively high enzyme concentration, whereas the use of lower amounts of enzyme or shorter incubation times predominantly resulted in accumulation of H3K9me1 (data not shown). There was no detectable activity toward H3K4me3 and H4K20me3, and only weak activity toward H3K27me3. Under similar assay conditions, recombinant Jmjd2a, Jmjd2b, and Jmjd2c removed only one methyl group from H1.4K26me3 peptides (Fig. 6*B*), again consistent with their ability to convert H3K9me3 to the dimethyl state *in vitro* (47). The addition of the iron chelating agent deferoxamine abolished the production of H1.4K26me2 (Fig. 6*B*). We also examined the enzymatic activity of recombinant mouse Lsd1 and *Drosophila* Lid proteins, which were shown to demethylate H3K4me1, or -me2 and me3, respectively (34, 46). We did not detect H1K26 demethylation by these enzymes under conditions wherein H3K4 peptide

demethylation was observed (data not shown). These results indicate that in addition to being H3K9me3-specific JMJD2 subfamily members are also H1.4K26-specific demethylases.

To test if JMJD2 proteins demethylate H1.4K26 in a cellular context we took advantage of a previously generated NIH3T3 cell line with stably integrated inducible Jmjd2b (35). In contrast to the host cell line, induction of Jmjd2b exhibited a ~4-fold reduction in H3K9me3 levels concomitant with increased H3K9me1 levels (Fig. 6*C*). Importantly, we also detected a reduction in H1.4K26me2/3 levels, but no significant increase in global H1.4K26me1 levels. This could be due to the high basal levels of H1.4K26me1 relative to those of H1.4K26me2/3. Given that mouse and human JMJD2 members are highly conserved we next assessed the ability of ectopic JMJD2 proteins to target H1.4K26 in a human cell system. We transiently transfected 293T cells with human JMJD2D, either the wild type or point mutant in its catalytic domain (H192A; described in Ref. 48). Only functional JMJD2D reduced global H1.4K26me2/3 levels and, consistent with earlier studies (49, 50), those of H3K9me2 (Fig. 6*D*). Taken together, we conclude that the mammalian family of JMJD2 proteins is responsible for the enzymatic turnover of H1.4K26 methylation *in vivo*.

DISCUSSION

Our data show that H1.4K26 is subject to dynamic methylation and that G9a is partially responsible for this process. G9a is highly homologous to another HKMT termed GLP/EuHMTase1 (51) both of which were shown to exhibit specificity for H3K9. For the purpose of this study we focused on G9a but it is likely that GLP also targets H1.4K26. Indeed, we identified GLP in our purification of H1.4K26 HKMT activity (supplemental Table S1) and G9a and GLP were shown previously to function in a heteromeric complex with both enzymes contributing to global H3K9me1 and -me2 (40). A recent report utilized SPOT array technology (described in Refs. 52 and 53) to identify G9a substrates on the basis of a G9a-target consensus sequence. H1.4K26 was identified among potential G9a substrates in the context of synthetic peptides (54). We have used an unbiased approach to identify H1.4K26-specific HKMTs. We clarified that G9a specifically methylates H1.4K26 using peptides and full-length recombinant proteins with or without the presence of core histones. Importantly, we demonstrated methylation of H1.4K26 by G9a *in vivo* using cell biological, genetic, and pharmacological approaches.

Recently, it was shown that the G9a and GLP ankyrin repeats recognize H3K9me1/2. It was speculated that one enzyme of the G9a-GLP complex recognizes the modification, whereas the other places the mark (55). Given the similarity of the residues surrounding H3K9 and H1.4K26 we suspect that the ankyrin repeats also recognize H1.4K26me2. Should this be the case, it is possible that the G9a-GLP complex might recognize H1.4K26me2 and subsequently methylate H3K9 within the same chromatosome or recognize H3K9me1/2 to methylate H1.4K26. Because G9a also methylates free H1.4 it is possible that binding of H1.4K26me2 to the ankyrin repeats provides a means by which G9a promotes its recruitment to chromatin. We found that G9a impacts H1 occupancy on promoter regions (Fig. 4, *D* and *E*) and it will be interesting to investigate in future studies if a mutation in the ankyrin repeats that is deficient for histone methyl-lysine binding affects H1-recruitment to chromatin.

The linker histone H1 was believed to constitute chromatin in a 1:1 ratio with core histone octamers. However, recent data demonstrated that H1 is not omnipresent but in certain instances subject to localized recruitment to establish facultative heterochromatin (recently discussed by Ref. 23). Moreover, genome-wide binding data illustrated that histone H1 is present predominantly over repressed genes and intergenic regions, whereas it is absent and replaced by PARP-1 along active genes (56). Therefore, it is likely that mechanisms are in place to deposit H1 or to exchange other chromatin binding factors with H1. Covalent modifications on core histones and the linker histone might affect such processes as recently demonstrated by studies showing that the presence or absence of H2A monoubiquitination affects H1 deposition (57, 58). H1.4K26me2 is recognized by several chromatin binding factors (Fig. 5, *A* and *B*) that might assist in its recruitment or increase its residence time on chromatin, thereby facilitating alterations of the chromatin structure. Important in this context is our finding that H1.4K26 methylation is enzymatically reversible. Members of the JMJD2 subfamily of H3K9/H3K36-specific demethylases have now been shown to target H1.4K26 as well. It was proposed that JMJD2 proteins regulate gene expression by locally altering histone methylation states. Demethylation of H1.4K26 would diminish the ability of repressive effector proteins like HP1 and L3MBTL1 to remain on chromatin and might also increase H1.4 mobility. Consequently, H1.4K26 demethylation by JMJD2 proteins would contribute to transcriptional activation.

We previously found that H1.4K26 is methylated by the H3K27-specific HKMT EZH2/PRC2 and here we have shown that the H3K9-specific HKMT G9a methylates H1.4K26 *in vitro* and *in vivo*. Several H3K9-HKMTs in addition to G9a are known in mammalian organisms and given the amino acid sequence similarity around H3K9, H3K27, and H1.4K26 it will be interesting to examine which of these histone methyltransferases, if any, have the potential to methylate H1.4K26. Previous reports and this study revealed that JMJD2 proteins target multiple sites including H1.4K26 but the H3K9-specific JMJD1 proteins and H3K27-specific demethylases like UTX did not demethylate H1.4K26 in our assays. This suggests that simple sequence similarity is not sufficient to define a recognition site. The crystal structural analysis of JMJD2A with methylated H3K9 and H3K36 peptides nicely illustrated distinct recognition mechanisms (59) and it would be interesting to see if a similar or distinct mechanism applies to H1.4K26 binding.

Acknowledgments—We thank Dr. Lynne Vales for critical reading of the manuscript. We also thank Drs. R. Jahnknecht, Y. Shinkai, Y. Nakatani, and Laura Pérez-Burgos for valuable reagents, S. Opravil, Drs. P. Lobel, S. Kubicek, G. Ammerer, and K. Mechtler for experimental support, and the NYU Protein Analysis Facility (NYU PAF) for routine protein identification. We thank Boehringer Ingelheim Pharmaceuticals, Inc. for providing compound BIX-01294.

REFERENCES

1. Langan, T. A. S., and Smith, L. K. (1967) *Fed. Proc.* **26,** 603
2. Wisniewski, J. R., Zougman, A., Kruger, S., and Mann, M. (2007) *Mol. Cell. Proteomics* **6,** 72–87
3. Pham, A. D., and Sauer, F. (2000) *Science* **289,** 2357–2360
4. Villar-Garea, A., and Imhof, A. (2008) *PLoS ONE* **3,** e1553
5. Ohe, Y., Hayasli, H., and Iwai, K. (1986) *J. Biochem.* (*Tokyo*) **100,** 359–368
6. Garcia, B. A., Joshi, S., Thomas, C. E., Chitta, R. K., Diaz, R. L., Busby, S. A., Andrews, P. C., Ogorzalek Loo, R. R., Shabanowitz, J., Kelleher, N. L., Mizzen, C. A., Allis, C. D., and Hunt, D. F. (2006) *Mol. Cell. Proteomics* **5,** 1593–1609
7. Kuzmichev, A., Jenuwein, T., Tempst, P., and Reinberg, D. (2004) *Mol. Cell* **14,** 183–193
8. Vaquero, A., Scher, M., Lee, D., Erdjument-Bromage, H., Tempst, P., and Reinberg, D. (2004) *Mol. Cell* **16,** 93–105
9. Ramón, A., Muro-Pastor, M. I., Scazzocchio, C., and Gonzalez, R. (2000) *Mol. Microbiol.* **35,** 223–233
10. Escher, D., and Schaffner, W. (1997) *Mol. Gen. Genet.* **256,** 456–461
11. Barra, J. L., Rhounim, L., Rossignol, J. L., and Faugeron, G. (2000) *Mol. Cell. Biol.* **20,** 61–69
12. Fan, Y., Sirotkin, A., Russell, R. G., Ayala, J., and Skoultchi, A. I. (2001) *Mol. Cell. Biol.* **21,** 7933–7943
13. Sirotkin, A. M., Edelmann, W., Cheng, G., Klein-Szanto, A., Kucherlapati, R., and Skoultchi, A. I. (1995) *Proc. Natl. Acad. Sci. U. S. A.* **92,** 6434–6438
14. Lin, Q., Sirotkin, A., and Skoultchi, A. I. (2000) *Mol. Cell. Biol.* **20,** 2122–2128
15. Fan, Y., Nikitina, T., Zhao, J., Fleury, T. J., Bhattacharyya, R., Bouhassira, E. E., Stein, A., Woodcock, C. L., and Skoultchi, A. I. (2005) *Cell* **123,** 1199–1212
16. Fan, Y., Nikitina, T., Morin-Kensicki, E. M., Zhao, J., Magnuson, T. R., Woodcock, C. L., and Skoultchi, A. I. (2003) *Mol. Cell. Biol.* **23,** 4559–4572
17. Woodcock, C. L. (2006) *Curr. Opin. Struct. Biol.* **16,** 213–220
18. Woodcock, C. L., Skoultchi, A. I., and Fan, Y. (2006) *Chromosome Res.* **14,** 17–25
19. Tremethick, D. J. (2007) *Cell* **128,** 651–654
20. Robinson, P. J., and Rhodes, D. (2006) *Curr. Opin. Struct. Biol.* **16,** 336–343
21. Alami, R., Fan, Y., Pack, S., Sonbuchner, T. M., Besse, A., Lin, Q., Greally, J. M., Skoultchi, A. I., and Bouhassira, E. E. (2003) *Proc. Natl. Acad. Sci. U. S. A.* **100,** 5920–5925
22. Koop, R., Di Croce, L., and Beato, M. (2003) *EMBO J.* **22,** 588–599
23. Trojer, P., and Reinberg, D. (2007) *Mol. Cell* **28,** 1–13
24. Godde, J. S., and Ura, K. (2008) *J. Biochem.* **143,** 287–293
25. Tuck, M. T., Farooqui, J. Z., and Paik, W. K. (1985) *J. Biol. Chem.* **260,** 7114–7121
26. Syed, S., Rajpurohit, R., Kim, S., and Paik, W. K. (1992) *J. Protein Chem.* **11,** 239–246
27. Allis, C. D., Berger, S., Jenuwein, T., Kouzarides, T., Pillus, L., Reinberg, D., Roth, S., Shi, Y., Shiekhattar, R., Shilatifard, A., Cote, J., Workman, J., and Zhang, Y. (2007) *Cell* **131,** 633–636
28. Kuzmichev, A., Margueron, R., Vaquero, A., Preissner, T. S., Scher, M., Kirmizis, A., Ouyang, X., Brockdorff, N., Abate-Shen, C., Farnham, P., and Reinberg, D. (2005) *Proc. Natl. Acad. Sci. U. S. A.* **102,** 1859–1864
29. Martin, C., Cao, R., and Zhang, Y. (2006) *J. Biol. Chem.* **281,** 8365–8370
30. Dignam, J. D., Martin, P. L., Shastry, B. S., and Roeder, R. G. (1983) *Methods Enzymol.* **101,** 582–598
31. Perez-Burgos, L., Peters, A. H., Opravil, S., Kauer, M., Mechtler, K., and Jenuwein, T. (2004) *Methods Enzymol.* **376,** 234–254
32. Peters, A. H., Kubicek, S., Mechtler, K., O'Sullivan, R. J., Derijck, A. A., Perez-Burgos, L., Kohlmaier, A., Opravil, S., Tachibana, M., Shinkai, Y., Martens, J. H., and Jenuwein, T. (2003) *Mol. Cell* **12,** 1577–1589
33. Nishioka, K., and Reinberg, D. (2003) *Methods* **31,** 49–58
34. Rudolph, T., Yonezawa, M., Lein, S., Heidrich, K., Kubicek, S., Schafer, C., Phalke, S., Walther, M., Schmidt, A., Jenuwein, T., and Reuter, G. (2007) *Mol. Cell* **26,** 103–115
35. Fodor, B. D., Kubicek, S., Yonezawa, M., O'Sullivan, R. J., Sengupta, R., Perez-Burgos, L., Opravil, S., Mechtler, K., Schotta, G., and Jenuwein, T. (2006) *Genes Dev.* **20,** 1557–1562
36. Trojer, P., Li, G., Sims, R. J., 3rd, Vaquero, A., Kalakonda, N., Boccuni, P., Lee, D., Erdjument-Bromage, H., Tempst, P., Nimer, S. D., Wang, Y. H., and Reinberg, D. (2007) *Cell* **129,** 915–928
37. Tachibana, M., Sugimoto, K., Fukushima, T., and Shinkai, Y. (2001) *J. Biol. Chem.* **276,** 25309–25317
38. Patnaik, D., Chin, H. G., Esteve, P. O., Benner, J., Jacobsen, S. E., and Pradhan, S. (2004) *J. Biol. Chem.* **279,** 53248–53258
39. Tachibana, M., Sugimoto, K., Nozaki, M., Ueda, J., Ohta, T., Ohki, M., Fukuda, M., Takeda, N., Niida, H., Kato, H., and Shinkai, Y. (2002) *Genes Dev.* **16,** 1779–1791
40. Tachibana, M., Ueda, J., Fukuda, M., Takeda, N., Ohta, T., Iwanari, H., Sakihama, T., Kodama, T., Hamakubo, T., and Shinkai, Y. (2005) *Genes Dev.* **19,** 815–826
41. Kubicek, S., O'Sullivan, R. J., August, E. M., Hickey, E. R., Zhang, Q., Teodoro, M. L., Rea, S., Mechtler, K., Kowalski, J. A., Homon, C. A., Kelly, T. A., and Jenuwein, T. (2007) *Mol. Cell* **25,** 473–481
42. Roopra, A., Qazi, R., Schoenike, B., Daley, T. J., and Morrison, J. F. (2004) *Mol. Cell* **14,** 727–738
43. Sarcevic, B., Spagnoli, G. C., Terracciano, L., Schultz-Thater, E., Heberer, M., Gamulin, M., Krajina, Z., Oresic, T., Separovic, R., and Juretic, A. (2003) *Oncology* **64,** 443–449
44. Wozniak, R. J., Klimecki, W. T., Lau, S. S., Feinstein, Y., and Futscher, B. W. (2007) *Oncogene* **26,** 77–90
45. Daujat, S., Zeissler, U., Waldmann, T., Happel, N., and Schneider, R. (2005) *J. Biol. Chem.* **280,** 38090–38095
46. Lee, N., Zhang, J., Klose, R. J., Erdjument-Bromage, H., Tempst, P., Jones, R. S., and Zhang, Y. (2007) *Nat. Struct. Mol. Biol.* **14,** 341–343
47. Whetstine, J. R., Nottke, A., Lan, F., Huarte, M., Smolikov, S., Chen, Z., Spooner, E., Li, E., Zhang, G., Colaiacovo, M., and Shi, Y. (2006) *Cell* **125,** 467–481
48. Cloos, P. A., Christensen, J., Agger, K., Maiolica, A., Rappsilber, J., Antal, T., Hansen, K. H., and Helin, K. (2006) *Nature* **442,** 307–311
49. Shin, S., and Janknecht, R. (2007) *Biochem. Biophys. Res. Commun.* **359,** 742–746
50. Shin, S., and Janknecht, R. (2007) *Biochem. Biophys. Res. Commun.* **353,** 973–977
51. Ogawa, H., Ishiguro, K., Gaubatz, S., Livingston, D. M., and Nakatani, Y. (2002) *Science* **296,** 1132–1136
52. Hilpert, K., Winkler, D. F., and Hancock, R. E. (2007) *Nature Protoc.* **2,** 1333–1349
53. Trojer, P., and Reinberg, D. (2008) *Nat. Chem. Biol.* **4,** 332–334
54. Rathert, P., Dhayalan, A., Murakami, M., Zhang, X., Tamas, R., Jurkowska, R., Komatsu, Y., Shinkai, Y., Cheng, X., and Jeltsch, A. (2008) *Nat. Chem. Biol.* **4,** 344–346
55. Collins, R. E., Northrop, J. P., Horton, J. R., Lee, D. Y., Zhang, X., Stallcup, M. R., and Cheng, X. (2008) *Nat. Struct. Mol. Biol.* **15,** 245–250
56. Krishnakumar, R., Gamble, M. J., Frizzell, K. M., Berrocal, J. G., Kininis, M., and Kraus, W. L. (2008) *Science* **319,** 819–821
57. Jason, L. J., Finn, R. M., Lindsey, G., and Ausio, J. (2005) *J. Biol. Chem.* **280,** 4975–4982
58. Zhu, P., Zhou, W., Wang, J., Puc, J., Ohgi, K. A., Erdjument-Bromage, H., Tempst, P., Glass, C. K., and Rosenfeld, M. G. (2007) *Mol. Cell* **27,** 609–621
59. Ng, S. S., Kavanagh, K. L., McDonough, M. A., Butler, D., Pilka, E. S., Lienard, B. M., Bray, J. E., Savitsky, P., Gileadi, O., von Delft, F., Rose, N. R., Offer, J., Scheinost, J. C., Borowski, T., Sundstrom, M., Schofield, C. J., and Oppermann, U. (2007) *Nature* **448,** 87–91